Hindawi
Mathematical Problems in Engineering
Volume 2022, Article ID 2906535, 10 pages
https://doi.org/10.1155/2022/2906535

Research Article

A Novel Low-Velocity Impact Region Identification Method for Cantilever Beams Using a Support Vector Machine

Fengde Wang,[1] **Yongtian Kang**,[2,3] **Wensheng Xiao**,[3] **Changjiang Li**,[3] **and Qi Liu**[3,4]

[1]*College of Mechanical and Electronic Engineering, Shandong University of Science and Technology, Qingdao 266590, China*
[2]*China Classification Society Offshore Engineering Technology Centre, Tianjin 300450, China*
[3]*College of Mechanical and Electronic Engineering, China University of Petroleum (East China), Qingdao 266580, China*
[4]*School of Mechanical & Aerospace Engineering, Nanyang Technological University, Singapore 639798, Singapore*

Correspondence should be addressed to Qi Liu; qi.liu@ntu.edu.sg

Received 20 April 2022; Accepted 12 September 2022; Published 7 October 2022

Academic Editor: Junwei Ma

Damage induced by a low-velocity impact can reduce the stability and reliability of structures. In this study, a novel low-velocity impact region identification method based on the spectral peak frequency (SPF) and support vector machine (SVM) is proposed to identify the low-velocity impact regions on a steel cantilever beam. A low-velocity impact region identification system of the cantilever beam is established by applying fiber Bragg grating (FBG) sensors, and only 2 sensors are used in this system. The power spectral density functions of the impact response signal are smoothed using the linear weighting method to remove pseudospectral peak frequencies, and then, SPFs are extracted as the features. For 25 low-velocity impact regions with dimensions of 30 mm × 10 mm, the results show that the recognition rate obtained by the proposed method is 100% and the feature vector consisting of the first two SPFs with the largest amplitude has the highest recognition rate. Through the comparative study, it is found that the recognition rate of SVM is higher than that of the probabilistic neural network (PNN) and extreme learning machine (ELM) for low-velocity impact area recognition of cantilever beams. As a result, the low-velocity impact region identification method of this paper can be applied to the real-time health monitoring of cantilever beam structures.

1. Introduction

A cantilever beam is the basic component of complex structural systems, and damages induced by the low-velocity impact will weaken the strength of the structure and shorten its working life. To ensure the reliability and safety of structures, structural health monitoring technology has been developed to monitor the working condition of structures in real time. The structural health monitoring system mainly consists of sensors and data analysis systems, which can identify the damage area and quantify damage. For cantilever beam structural health monitoring, modal parameters and their spatial derivatives, structural parameters, and vibration response signals are frequently used to achieve the damage detection, localization, and quantitative analysis. Vibration mode changes are more correlated with structural damage; however, since high-order modes are difficult to measure accurately, Vafaei and Alih [1] proposed a damage identification method based on the artificial neural network and the first-order mode. To overcome the disadvantage of mode shapes being more difficult to be measured, Oliveira Filho et al. [2] performed some work to study the optimization of the sensor installation position on beam structures. Ghannadi and Kourehli [3] proposed a modal test analysis model to estimate unmeasured mode shapes for damage assessment of the cantilever beam. For noisy signals, a stationary wavelet transform was applied to separate the feature and noise, and the differences between modes were determined by continuous wavelet transform [4]. To eliminate irregularities and noises of the beam damage detection process, Masoumi and Ashory [5] proposed a uniform load surface (ULS) based on the flexibility matrix and

improved the obtained ULS by stationary wavelet transform. Derived from the fundamental mode shape, a curvature mode shape has been widely used in damage identification of beams, to overcome its susceptibility to measurement noise, Cao et al. [6] developed a synergy method using a wavelet transform and a Teager energy operator, and a mode shape curvature estimation method based on the damaged structure data has been developed to locate damage [7]. Since the natural frequency is much easier to measure than the mode and curvature, it has been used by some scholars to investigate the crack detection of cantilever beams [8–10]. More scholars applied the mode shape and natural frequency together for damage identification and location [11–15]. Flexibility is another key parameter for structure damage identification, the comparative study of vibration and wave propagation approaches based on the flexibility matrix of cantilever beams has been implemented [16], and a damage detection method based on a modal flexibility matrix has been proposed for the cantilever beam structures [17]. By combining natural frequency and flexibility, Dahak et al. [18] developed an algorithm to identify the damage regions in the cantilever beam. According to the experimental data of damaged and undamaged beams, Khatir et al. [19] formed an objective function with the changes of natural frequencies and proposed a damage detection method based on the particle swarm optimization algorithm, and their method can also quantify damage. Hu and Zhang [20] calculated the stiffness reduction of the damage beam using the improved beetle antennae search algorithm and constructed a damage index that can track the curvature changes of modes.

Due to the basic idea that the damage-induced changes of structures will cause detectable signals of vibration responses, some scholars have developed several damage detection methods using the measured signal [21–25]. Zai et al. [26] investigated the changes in frequency, damping, and vibration response amplitude under thermomechanical loads and proposed a damage quantification method for cantilever beams. With the development of intelligent algorithms and signal processing technologies, bispectral analysis [27], neural network [27, 28], spatial wavelet analysis [29], full wavelet scalogram [28], metaheuristic algorithm [30], Bayesian parameter estimation [31], and deep learning [32] have shown significant promise in the damage detection of cantilever beams.

Impacts occurring at velocities 1 to 10 m/s are treated as a low-velocity impact (LVI) by Cantwell and Morton [33], and LVI often creates damage with dent depths lower than barely visible impact damage, which attracted some scholars to investigate it. Jang et al. [34] proposed a real-time impact identification algorithm for the composite flat plate under the low-velocity impact load, and Qi et al. [35] investigated the effects of impact velocity on the performance of an expansion tube by the experiment method and numerical simulation. In view of the application of the support vector machine in pattern recognition problems [36–38], we put our focus on the low-velocity impact region identification method of cantilever beams. In this study, two fiber Bragg grating (FBG) sensors are installed on the cantilever beam to collect impact response signals and the power spectral density (PSD) is obtained using the Fourier transform method. Based on the spectral peak frequencies (SPFs) of PSD and SVM, we proposed a low-velocity impact region identification method. The identification rate of this method is 100%, which can be applied to real-time health monitoring of cantilever beams.

The paper is structured as follows: Section 2 illustrates the relative theories of the research. The details of a low-velocity impact identification system of cantilever beams are presented in Section 3. In Section 4, the proposed algorithm is introduced briefly. Then, the method is used to identify the impact regions, and the results are discussed in Section 5. Finally, Section 6 gives the conclusions.

2. Relative Theories

2.1. Working Principles of an FBG Sensor. An FBG sensor satisfies the Bragg condition as follows:

$$\lambda = 2n_{\text{neff}}\Lambda, \tag{1}$$

where λ is the Bragg wavelength, n_{neff} is the effective refractive index of fiber grating, and Λ is the Bragg grating spacing.

When the measured physical quantities (e.g., temperature and strain) acting on the fiber grating change, the corresponding changes of n_{neff} and Λ will result in the drift of λ, and it changes linearly. Therefore, the information of the measured physical quantity can be obtained by measuring the drift of λ. In the laboratory environment, the temperature does not change much and can be regarded as a constant value. Then, the variation of λ is generated only by the change of strain. Thus, the shift of λ can be formulated as follows:

$$\Delta\lambda_{\varepsilon} = \lambda\varepsilon\left(1 - P_{\varepsilon}\right), \tag{2}$$

where P_{ε} is the effective elasto-optical coefficient, and ε is strain.

When an FBG sensor is used for structural health monitoring of the cantilever beam, the strain response pattern of the beam changes as the impact region changes, which subsequently causes the change of λ.

2.2. Support Vector Multiple Classification Algorithm. SVM is a structural risk minimization method developed based on statistical learning theory, which can solve classification and pattern recognition problems. Since the size of the sample has little significant effect on the performance of SVM, the support vector machine also has high efficiency and accuracy when processing large sample data.

The sample data and categories are labeled as $\{p_i, q_i\}$, $i = 1, 2, \ldots, s$, $q_i \in \{-1, 1\}$, where s is the number of the sample data. For soft margin classification, the original problem of SVM is determined as follows:

$$\begin{cases} \min \quad \dfrac{1}{2}\|\omega\|^2 + c\displaystyle\sum_{i=1}^{s}\varepsilon_i \\ \\ \text{s.t.} \quad q_i\left(\omega p + b^*\right) \geq 1 - \varepsilon_i\left(\varepsilon_i \geq 0\right). \end{cases} \tag{3}$$

In (3), ω is the weight vector, b^* is the bias vector, ε_i is the slack factor, and c is the penalty parameter. Then, the classification problems can be expressed as the dual optimization problem:

$$\begin{cases} \min \quad \frac{1}{2}\sum_{i=1}^{j}\sum_{j=1}^{s} q_i q_j \alpha_i \alpha_j K\left(p_i, p_j\right) - \sum_{i=1}^{s} \alpha_i \\ \\ \text{s.t.} \quad \sum_{i=1}^{s} \alpha_i q_i = 0 \left(0 \le \alpha_i \le c\right). \end{cases} \tag{4}$$

In (4), α_i is the Lagrange multiplier and $K(p_i, p_j)$ is a kernel function. The main forms of the kernel function are linear function, polynomial function, Gaussian function, and radial basis function (RBF). Since RBF has faster learning speed and stronger classification ability, we choose it as the kernel function in this study, and the expression of RBF is presented in (5), where ξ is the kernel parameter.

$$K\left(p_i, p_j\right) = \exp\left(-\xi \left\| p_i - p_j \right\|^2\right). \tag{5}$$

According to the sample data, the classification results can be obtained by the following decision function:

$$f(p) = \operatorname{sgn}\left(\sum_{i=1}^{s} \alpha_i^* q_i K\left(p_i, p_j\right) + b^*\right). \tag{6}$$

3. Low-Velocity Impact Region Identification System

The low-velocity impact region identification system consists of a fiber grating sensing interrogator (Micron Optics si155 of Micron Optics Inc), a steel cantilever beam, two FBG sensors, and a computer, and Figure 1 illustrates the experimental site. With a wavelength accuracy of 2pm/3pm, Micron Optics si155 has two parallel channels, each with a bandwidth of 80 nm, which enables simultaneous full-spectrum scanning at 5 kHz. si155 is equipped with a high-power, low-noise, ultralarge bandwidth scanning laser source to ensure wavelength accuracy of scanning. It enables fast full-spectrum data acquisition and low latency access to data in closed-loop feedback applications, and it is suitable for Bragg gratings, long-period gratings, and Fabry–Perot optical fiber sensors. si155 is equipped with special demodulation software ENLIGHT. Its functions include data acquisition, calculation, and analysis of fiber grating sensor networks, and the software can convert optical wavelength parameters into strain, temperature, acceleration, pressure, etc.

Figure 2 shows a schematic diagram of the low-velocity impact localization system. The dimensions of the steel cantilever beam are 750 mm × 10 mm × 2 mm, and it is evenly divided into 25 small regions of 30 mm × 10 mm along the axial direction in the experiment. The grating lengths of the two FBG sensors are 10 mm, and the Bragg wavelength values are 1549.859 nm and 1549.958 nm, respectively. FBG sensors are mounted on each end of the beam at coordinates (0, 105 mm) and (0, 645 mm). A steel ball weighing 36 g was used as the impact device, and in the experiment, it hit the beam vertically in a free-fall manner.

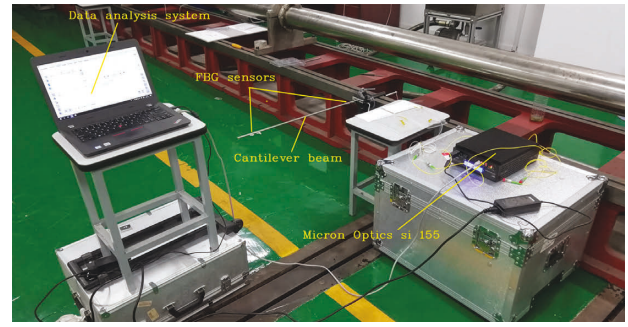

Figure 1: A site diagram of the low-velocity impact test of the steel cantilever beam.

4. Low-Velocity Impact Region Identification Method

4.1. Feature Extraction. To identify the impact regions of the cantilever beam, the SPFs of the PSD of the impact response signal are extracted as features. The impact response signals collected by two FBG sensors are shown in Figure 3 Then, the PSD of the impact response signals are obtained by the Fourier transform, as shown in Figures 4 and 5. Obviously, there are multiple pseudospectral frequencies near spectral peak frequencies. To extract the main features and ensure the validity of the features, PSD needs to be processed to remove the pseudospectral peak frequencies. In this research, we chose the smoothing process method to filter the pseudospectral peak frequencies. Through the comparative study, it is found that the weighted linear fitting method has a better processing effect on PSD.

For the weighted linear fitting method, the window length has a significant effect on data processing results, which indicates that the processing results are severely distorted (Figure 6) when the window length is less than 1. Therefore, the window length should be greater than 1 when weighted linear fitting is used to process impact response signals. The window length is set to 15 after executing extensive tests, and the power spectral density of impact response signals after the smoothing process are presented in Figures 4 and 5.

The impact signals collected by two FBG sensors in each region were randomly selected to study the relationship between the characteristics of the signal and the impact regions. PSD of signals in region 2, region 5, region 8, region 11, region 14, region 17, region 20, and region 23 were selected to illustrate our method, as shown in Figures 7–9. PSD shows that the main frequencies vary with the impact region, and the FBG 2 sensor collects low-order spectral peak frequencies of the signal.

As shown in Figure 8, the main frequency of the impact response signal collected by using the FBG 2 sensor is 5.49 Hz in region 2, region 5, region 8, region 11, and region

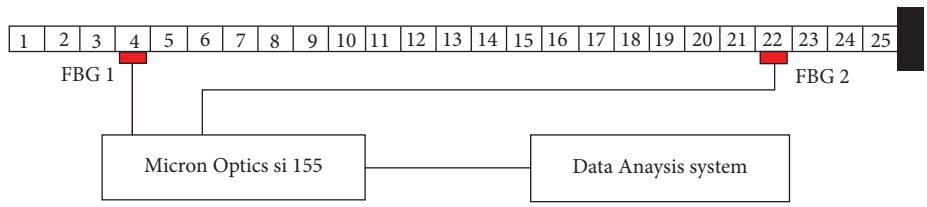

Figure 2: A schematic diagram of the low-velocity impact localization system.

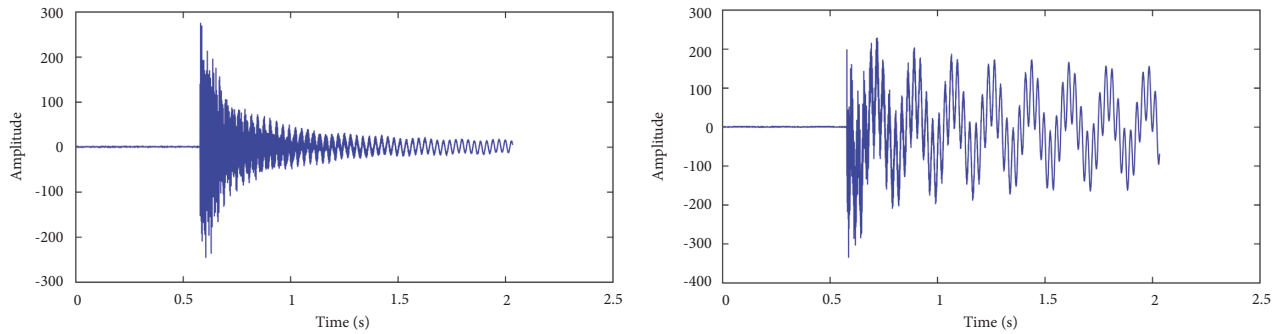

Figure 3: Original signals of FBG sensors in region 13: (a) FBG 1 signal and (b) FBG 2 signal.

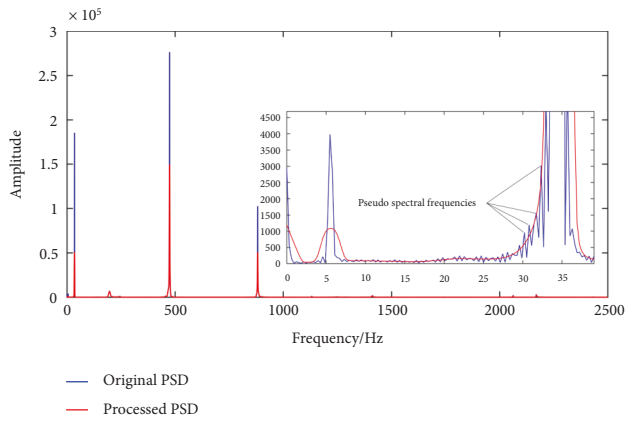

Figure 4: Power spectral density of the FBG 1 signal in region 13.

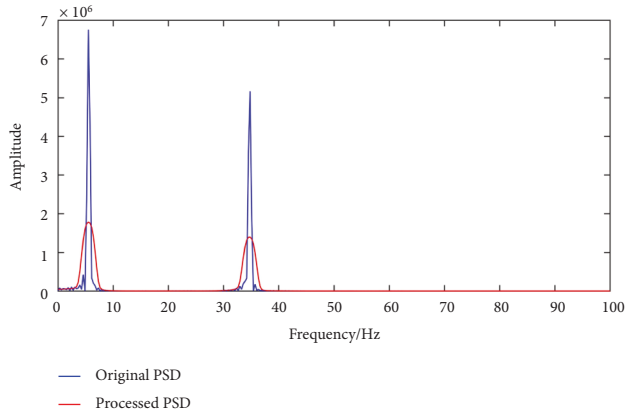

Figure 5: Power spectral density of the FBG 2 signal in region 13.

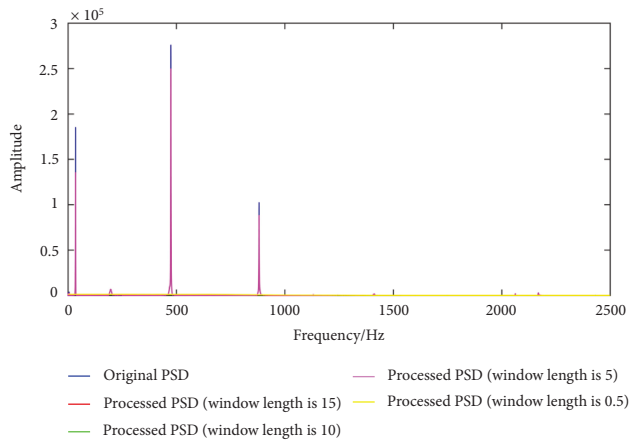

Figure 6: Power spectral density of the FBG 1 signal in region 13 at different window lengths.

14, and 34.79 Hz is the main frequency in region 17 and region 20. Therefore, according to spectral peak frequency characteristics of impact response signals, the impact range can be roughly determined: when the main frequency is 5.49 Hz, the impact region is close to the free end; when the main frequency is 34.79 Hz, the impact region is located in the middle of the cantilever beam; when the main frequency is 881.4 Hz and other high spectral peak frequencies, the impact region is distributed near the fixed end of the cantilever beam, and Figure 9 illustrates the relevant results.

Comparing Figures 7–9, it is found that more spectral peak frequencies of the impact response signal are excited in the region close to the fixed end, which indicates that it is easier to achieve high-precision location of impact regions. Based on the above research results, the first three spectral

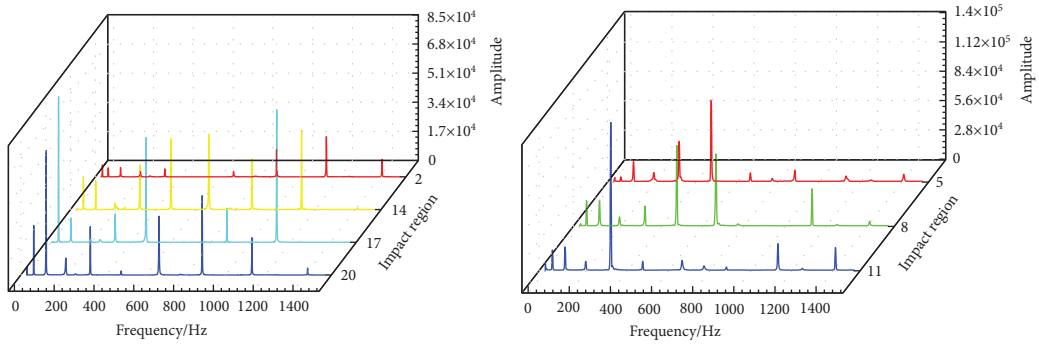

Figure 7: Amplitude-frequency characteristics of the FBG 1 sensor signal.

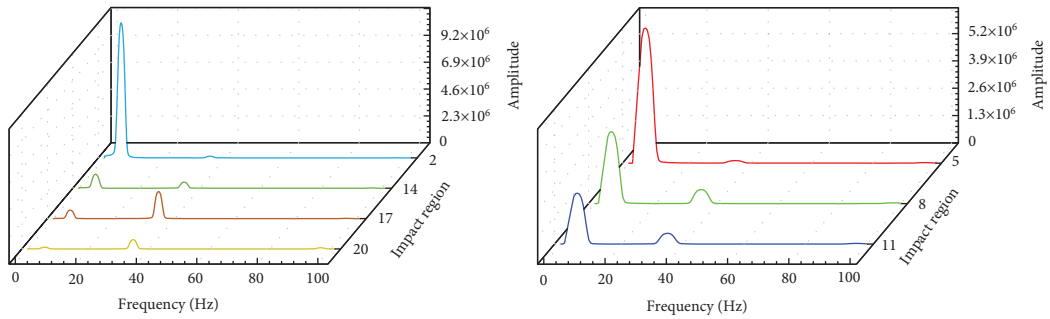

Figure 8: Amplitude-frequency characteristics of the FBG 2 sensor signal.

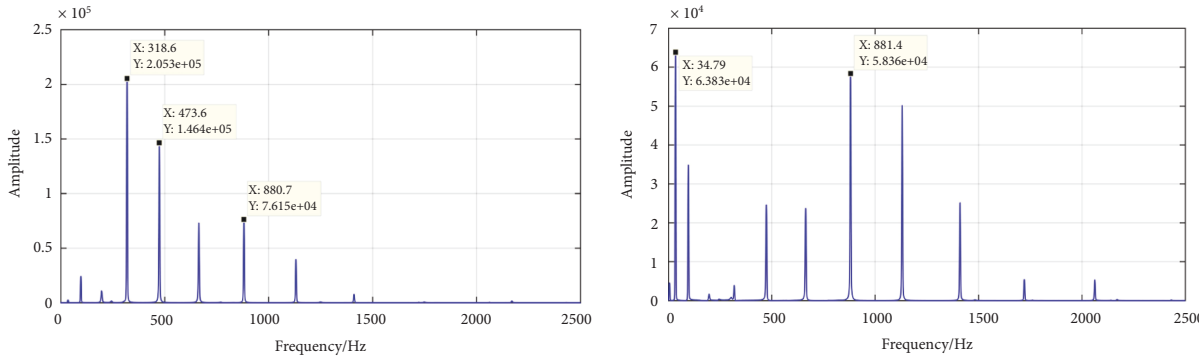

Figure 9: Amplitude-frequency characteristics impact signal in region 23. (a) Power spectrum of the FBG 1 signal and (b) power spectrum of the FBG 2 signal.

peak frequencies with the highest power amplitude of the FBG 1 signal and the first two spectral peak frequencies with the highest power amplitude of the FBG 2 signal were selected as features to identify the impact regions.

4.2. Identification Method Based on SVM. Aiming at identifying the low-velocity impact regions on the cantilever beam, m regions are divided on the cantilever beam as the impact regions to be identified, and an SVM model is established by treating each region as one category. The m categories are labeled as $R = \{1, 2, \ldots, m\}$, and then, the low-velocity impact region identification problem is transformed into a classification problem with m categories. The sample data are defined as $\{(x_i, y_i), i = 1, 2, \ldots, m\}$ and $y_i \in R$. x_i represents the signal characteristics monitored by n sensors, $x_i = \{F_{i1}, F_{i2}, \ldots, F_{in}\}$, and the signal monitored using a single FBG sensor is characterized by $F_{in} = \{f_1, f_2, \ldots, f_k\}$. In this study, we take the PSD of the strain response signal as the characteristic and f_k is the amplitude of PSD. The features of the impact response signals from different regions are used as input to the SVM model, and the impact regions are output. Then, the training and testing processes of the SVM model are constructed. In [39], we can note that the computational complexity of SVM in the training process is $O(k{\cdot}m^2)$ and the computational complexity of SVM in the testing process is $O(k{\cdot}Ns)$, where Ns is the number of the support vectors.

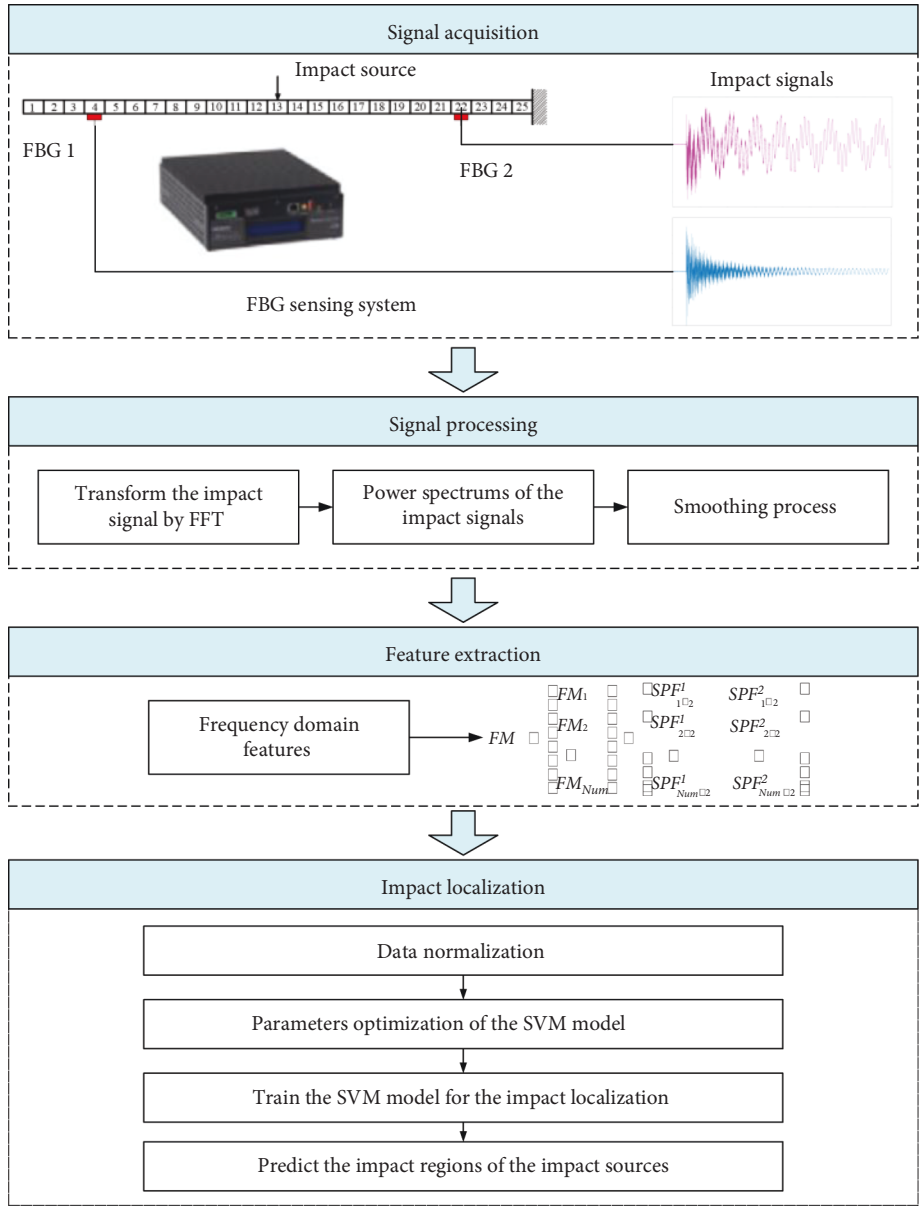

Figure 10: The flowchart of the low-velocity impact region identification procedure for the cantilever beam.

4.3. Low-Velocity Impact Region Identification Procedure. Based on SPF and SVM, the low-velocity impact region identification method of the cantilever beam is established in this study, and our method mainly has three steps: (a) signal preprocessing; (b) feature extraction; (c) impact region identification. Figure 10 illustrates the flowchart of our method.

The details of the low-velocity impact region identification method are given as follows:

Step 1: The impact response signal obtained from the fiber grating sensing system is processed by applying Fourier transformation to get the PSD of the signal. Then, PSD is smoothed by the weighted linear fitting method.

Step 2: The SPFs of smoothed PSD are selected as features. Each region is labeled by four features which are composed of the first two peak frequencies with the maximum amplitude of the smoothed PSD of the FBG 1 signal and the first two peak frequencies with the maximum amplitude of the smoothed PSD of the FBG 2 signal. Then, the feature matrix FM can be expressed as follows:

$$\mathrm{FM} = \begin{bmatrix} \mathrm{FM}_1 \\ \mathrm{FM}_2 \\ \vdots \\ \mathrm{FM}_{\mathrm{Num}} \end{bmatrix} = \begin{bmatrix} \mathrm{SPF}^1_{1\times 2} & \mathrm{SPF}^2_{1\times 2} \\ \mathrm{SPF}^1_{2\times 2} & \mathrm{SPF}^2_{2\times 2} \\ \vdots & \vdots \\ \mathrm{SPF}^1_{\mathrm{Num}\times 2} & \mathrm{SPF}^2_{\mathrm{Num}\times 2} \end{bmatrix}. \quad (7)$$

Step 3: Low-velocity impact tests were carried out in 25 regions on the cantilever beam, respectively, and one group of feature samples obtained in the experiment

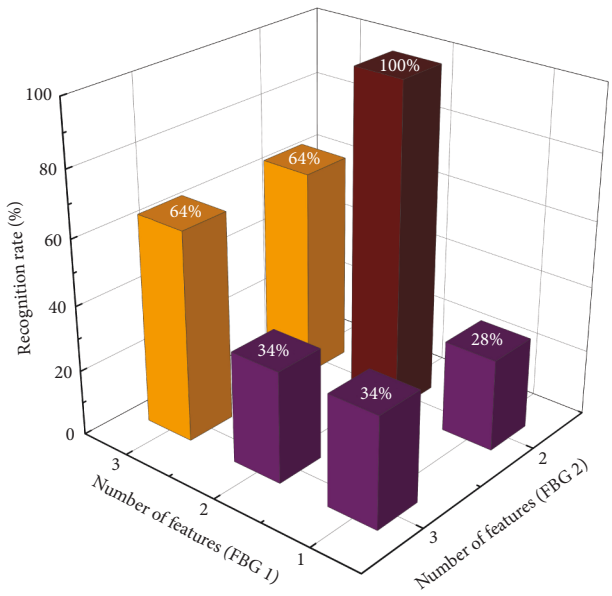

Figure 11: Recognition rate under different numbers of features.

was randomly selected as test samples, while the other samples were used as training samples. We take the SPFs of signals as the input to the SVM, and then, impact regions will be generated as the output of the SVM. The steel ball was used to impact 25 regions of the cantilever beam respectively, each area was impacted 3 times, and 3 groups of impact signals were obtained from each region. The SVM model was trained with the training sample set, and then, the recognition rate of the low-velocity impact region of the trained model was verified with the test sample set.

5. Results and Discussion

5.1. Parameter Setting. In the SVM, the form of the kernel mapping distribution of samples is mainly determined by the kernel parameter, while the penalty factor is mainly used to weigh the fitting ability and prediction ability of the algorithm. When the value of the kernel parameter is smaller and the penalty parameter is larger, the nonlinear fitting ability of the algorithm is stronger, but the training time increases. Smoothness decreases with the decrease of the kernel parameter, and generalization ability decreases with the increase of the penalty parameter. Therefore, it is necessary to determine the optimal combination of the kernel parameter and the penalty factor because the two parameters significantly affect the identification accuracy of SVM. The cross-validation method is an unbiased estimation of generalization errors, and it can effectively prevent overlearning phenomenon. It has both certain training accuracy and good generalization performance. Researchers have conducted many experiments using different learning techniques and a large data set, and the results showed that 10-fold is an appropriate choice to obtain the best error estimate [40–42]. In this study, based on the 10-fold cross-validation strategy, the grid search method was used to optimize the penalty factor, and the value of the penalty factor is determined to be 2.

5.2. Effect of the Number of FBG Sensors and the Number of Features. The number of FBG sensors and features was investigated in this research. First, only the SPFs of the FBG 1 sensor signal were used for identification, and the identification rate was 44% when we only used the SPF with the maximum amplitude; when the first two SPFs with the largest amplitude were used, the identification rate achieved 84%; the first three SPFs with the largest amplitude can achieve the 56% identification rate. The results show that it is reasonable to use the first two SPFs with the largest signal amplitude of the FBG 1 sensor for identification. According to the results of feature extraction mentioned above and combined with FBG 2 sensor signals, the identification rates under different numbers of features are studied, respectively. The research results are shown in Figure 11. The results show that the feature vectors constructed by using the first two SPFs with the largest amplitude of the FBG 1 signal and the first two SPFs with the largest amplitude of the FBG 2 signal can achieve the 100% identification rate. Therefore, the number of features corresponding to each region is 4.

5.3. Comparison of SVM and Other Algorithms. In order to verify the performance of SVM in the identification of low-velocity impact regions of cantilever beams, we used the SVM, least squares support vector machines (LS-SVM), probabilistic neural networks (PNN), and extreme learning machines (ELM) to identify impact regions, respectively. Figure 12 shows the recognition results of the above algorithms.

As shown in Figure 12, the identification rate of PNN is 92% and the identification rate of ELM is 84%, while both SVM and LS-SVM achieve the 100% identification rate. According to the identification results of PNN and ELM, it

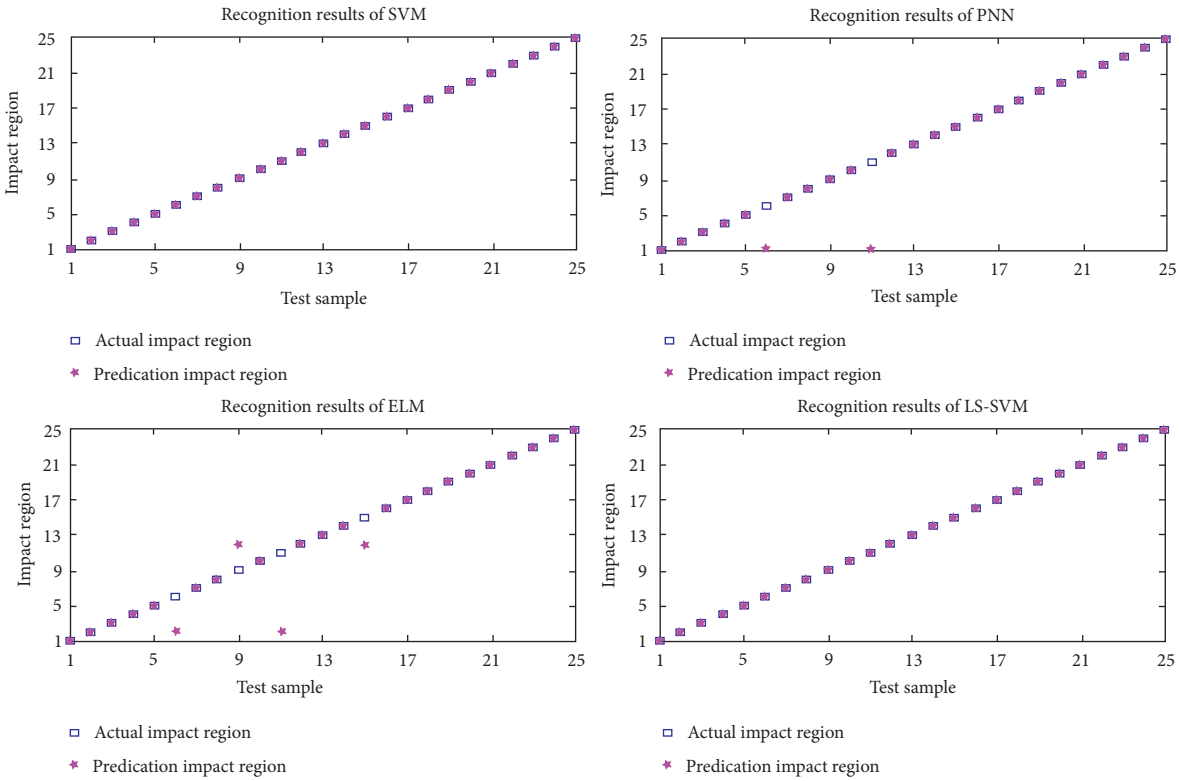

Figure 12: Recognition results of different algorithms.

can be concluded that the impact regions in the middle of the cantilever beam are more difficult to be identified. Based on the research results, it is speculated that the recognition accuracy of the impact regions can be further improved by adding sensors in the middle of the cantilever beam. The identification results in Figure 12 show that those areas near the fixed end of the cantilever beam are easier to identify, verifying the preliminary judgment in Section 4.1. For engineering applications, the calculation time of the algorithm should also be considered, and for 25 regions in this study, the average calculation time of SVM is 0.03987 s (30 times) and the average calculation time of LS-SVM is 0.28454 s (30 times). Therefore, we choose SVM to fulfill impact region identification. The results in this study are obtained based on the experimental data, and the quality of sample signals is relatively high. In practical application, many uncertain working conditions will be encountered, such as the sudden change in signal amplitude and the change in the signal type [43, 44]. The problems that may occur in the real-time application of the proposed algorithm are multisource impact and high-speed impact. Multisource impact can still be assumed as a single point impact in essence, and high-speed impact does not belong to the research scope of this paper.

6. Conclusions

A novel method to identify low-velocity impact regions of cantilever beams is proposed based on the spectral peak frequencies of PSD and SVM, and a low-velocity impact region identification system of cantilever beams based on an FBG sensor was established. The results show that the proposed method can accurately identify 25 regions of 30 mm × 10 mm on the cantilever beam with only two FBG sensors, and the recognition rate of this system is 100%. Therefore, it is feasible to use an FBG sensor to achieve low-velocity impact region identification of steel cantilever beams based on SVM with the spectral peak frequency feature. The proposed method in this paper can be used for real-time health monitoring of cantilever beam structures; however, the identification accuracy of the proposed method is not high enough, and it is more suitable for impact identification of large-scale structures. Aiming at the defect of insufficient precision, the optimization of sensor quantity and installation position should be further carried out. This study was conducted under laboratory conditions, where the experimental environment was more deterministic, making the signal characteristics more stable. However, in actual working conditions, both randomness and noise of the signal are enhanced, which makes it more difficult to identify the features of the signal. Therefore, in order to make our method applied and promoted in the field, it is necessary to carry out field experiments and research on impact region identification based on the field experimental data.

Data Availability

No data were used to support this study.

Conflicts of Interest

The authors declare that they have no conflicts of interest regarding publication of this paper.

Acknowledgments

This work was supported in part by the project from the Ministry of Industry and Information Technology of China under Grant CJ09N20, 2019GXB01-01-001.

References

[1] M. Vafaei and S. C. Alih, "Adequacy of first mode shape differences for damage identification of cantilever structures using neural networks," *Neural Computing & Applications*, vol. 30, no. 8, pp. 2509–2518, 2018.

[2] M. V. M. Oliveira Filho, J. E. P. Ipiña, and C. A. Bavastri, "Analysis of sensor placement in beams for crack identification," *Latin American Journal of Solids and Structures*, vol. 15, no. 11, p. e67, 2018.

[3] P. Ghannadi and S. S. Kourehli, "An effective method for damage assessment based on limited measured locations in skeletal structures," *Advances in Structural Engineering*, vol. 24, no. 1, pp. 183–195, 2021.

[4] R. Serra and L. Lopez, "Damage detection methodology on beam-like structures based on combined modal Wavelet Transform strategy," *Mechanics & Industry*, vol. 18, no. 8, p. 807, 2017.

[5] M. Masoumi and M. R. Ashory, "Damage identification from uniform load surface using continuous and stationary wavelet transforms," *Latin American Journal of Solids and Structures*, vol. 11, no. 5, pp. 738–754, 2014.

[6] M. Cao, M. Radzieński, W. Xu, and W. Ostachowicz, "Identification of multiple damage in beams based on robust curvature mode shapes," *Mechanical Systems and Signal Processing*, vol. 46, no. 2, pp. 468–480, 2014.

[7] S. M. H. Pooya and A. Massumi, "A novel and efficient method for damage detection in beam-like structures solely based on damaged structure data and using mode shape curvature estimation," *Applied Mathematical Modelling*, vol. 91, pp. 670–694, 2021.

[8] S. Moradi, P. Razi, and L. Fatahi, "On the application of bees algorithm to the problem of crack detection of beam-type structures," *Computers & Structures*, vol. 89, no. 23-24, pp. 2169–2175, 2011.

[9] S. A. Moezi, E. Zakeri, A. Zare, and M. Nedaei, "On the application of modified cuckoo optimization algorithm to the crack detection problem of cantilever Euler–Bernoulli beam," *Computers & Structures*, vol. 157, pp. 42–50, 2015.

[10] A. J. Choi and J. H. Han, "Frequency-based damage detection in cantilever beam using vision-based monitoring system with motion magnification technique," *Journal of Intelligent Material Systems and Structures*, vol. 29, no. 20, pp. 3923–3936, 2018.

[11] A. C. Altunışık, F. Y. Okur, and V. Kahya, "Modal parameter identification and vibration based damage detection of a multiple cracked cantilever beam," *Engineering Failure Analysis*, vol. 79, pp. 154–170, 2017.

[12] G. Samourgkanidis and D. Kouzoudis, "A pattern matching identification method of cracks on cantilever beams through their bending modes measured by magnetoelastic sensors," *Theoretical and Applied Fracture Mechanics*, vol. 103, Article ID 102266, 2019.

[13] V. Kahya, S. Karaca, F. Y. Okur, A. C. Altunışık, and M. Aslan, "Damage localization in laminated composite beams with multiple edge cracks based on vibration measurements," *Iranian Journal of Science and Technology, Transactions of Civil Engineering*, vol. 45, no. 1, pp. 75–87, 2021.

[14] Y. Jiang, N. Wang, and Y. Zhong, "A two-step damage quantitative identification method for beam structures," *Measurement*, vol. 168, Article ID 108434.

[15] S. S. B. Chinka, S. R. Putti, and B. K. Adavi, "Modal testing and evaluation of cracks on cantilever beam using mode shape curvatures and natural frequencies," *Structures*, vol. 32, no. 1, pp. 1386–1397, 2021.

[16] R. A. Tenenbaum, L. T. Stutz, and K. M. Fernandes, "Comparison of vibration and wave propagation approaches applied to assess damage influence on the behavior of Euler–Bernoulli beams," *Computers & Structures*, vol. 89, no. 19-20, pp. 1820–1828, 2011.

[17] S. H. Sung, K. Y. Koo, and H. J. Jung, "Modal flexibility-based damage detection of cantilever beam-type structures using baseline modification," *Journal of Sound and Vibration*, vol. 333, no. 18, pp. 4123–4138, 2014.

[18] M. Dahak, N. Touat, N. Benseddiq, and Benseddiq, "On the classification of normalized natural frequencies for damage detection in cantilever beam," *Journal of Sound and Vibration*, vol. 402, pp. 70–84, 2017.

[19] K. Dekemele, S. Khatir, M. Loccufier, T. Khatir, M. Abdel Wahab, and M. A. Wahab, "Crack identification method in beam-like structures using changes in experimentally measured frequencies and Particle Swarm Optimization," *Comptes Rendus Mecanique*, vol. 346, no. 2, pp. 110–120, 2018.

[20] Z. Hu and P. Zhang, "Damage identification of structures based on smooth orthogonal decomposition and improved beetle antennae search algorithm," *Advances in Civil Engineering*, vol. 202114 pages, Article ID 8857356, 2021.

[21] D. G. Kim and S. B. Lee, "Structural damage identification of a cantilever beam using excitation force level control," *Mechanical Systems and Signal Processing*, vol. 24, no. 6, pp. 1814–1830, 2010.

[22] F. Ghrib, L. Li, and P. Wilbur, "Damage identification of Euler–Bernoulli beams using static responses," *Journal of Engineering Mechanics*, vol. 138, no. 5, pp. 405–415, 2012.

[23] S. A. Ravanfar, H. A. Razak, Z. Ismail, and S. J. S. Hakim, "A hybrid procedure for structural damage identification in beam-like structures using wavelet analysis," *Advances in Structural Engineering*, vol. 18, no. 11, pp. 1901–1913, 2015.

[24] A. Theodosiou, M. Komodromos, and K. Kalli, "Carbon cantilever beam health inspection using a polymer fiber Bragg grating array," *Journal of Lightwave Technology*, vol. 36, no. 4, pp. 986–992, 2018.

[25] H. Zhu, H. Yu, F. Gao, S. Weng, Y. Sun, and Q. Hu, "Damage identification using time series analysis and sparse regularization," *Structural Control and Health Monitoring*, vol. 27, no. 9, Article ID e2554, 2020.

[26] B. A. Zai, M. A. Khan, K. A. Khan, and A. Mansoor, "A novel approach for damage quantification using the dynamic response of a metallic beam under thermo-mechanical loads," *Journal of Sound and Vibration*, vol. 469, Article ID 115134, 2020.

[27] M. Civera, L. Z. Fragonara, and C. Surace, "A novel approach to damage localisation based on bispectral analysis and neural network," *Smart Structures and Systems*, vol. 20, no. 6, pp. 669–682, 2017.

[28] J. Pacheco-Chérrez, A. Delgado-Gutiérrez, D. Cárdenas, and O. Probst, "Reliable damage localization in cantilever beams

using an image similarity assessment method applied to wavelet-enhanced modal analysis," *Mechanical Systems and Signal Processing*, vol. 149, Article ID 107335, 2020.

[29] A. Ghanbari Mardasi, N. Wu, and C. Wu, "Experimental study on the crack detection with optimized spatial wavelet analysis and windowing," *Mechanical Systems and Signal Processing*, vol. 104, pp. 619–630, 2018.

[30] B. Firouzi, A. Abbasi, and P. Sendur, "Improvement of the computational efficiency of metaheuristic algorithms for the crack detection of cantilever beams using hybrid methods," *Engineering Optimization*, vol. 54, no. 7, pp. 1236–1257, 2022.

[31] V. Kahya, F. Y. Okur, S. Karaca, A. C. Altunışık, and M. Aslan, "Multiple damage detection in laminated composite beams using automated model update," *Structures*, vol. 34, pp. 1665–1683, 2021.

[32] D. M. Onchis and G. R. Gillich, "Stable and explainable deep learning damage prediction for prismatic cantilever steel beam," *Computers in Industry*, vol. 125, Article ID 103359.

[33] W. J. Cantwell and J. Morton, "The impact resistance of composite materials-a review," *Composites*, vol. 22, no. 5, pp. 347–362, 1991.

[34] B. W. Jang, Y. G. Lee, J. H. Kim, Y. Y. Kim, and C. G. Kim, "Realtime impact identification algorithm for composite structures using fiber Bragg grating sensors," *Structural Control and Health Monitoring*, vol. 19, no. 7, pp. 580–591, 2012.

[35] Z. Qi, Y. Zhang, Y. Lin, R. Chen, and Y. Meng, "Dynamic response and energy absorption characteristics of expansion tubes under axial impact," *IEEE Access*, vol. 8, pp. 90528–90541, 2020.

[36] Q. Liu, L. Wu, F. Wang, and W. Xiao, "A novel support vector machine based on hybrid bat algorithm and its application to identification of low velocity impact areas," *IEEE Access*, vol. 8, pp. 8286–8299, 2020.

[37] Y. Wang, H. Tang, J. Huang, T. Wen, J. Ma, and J. Zhang, "A comparative study of different machine learning methods for reservoir landslide displacement prediction," *Engineering Geology*, vol. 298, Article ID 106544, 2022.

[38] J. Ma, Y. Wang, X. Niu, S. Jiang, and Z. Liu, "A comparative study of mutual information-based input variable selection strategies for the displacement prediction of seepage-driven landslides using optimized support vector regression," *Stochastic Environmental Research and Risk Assessment*, Springer, Berlin, Germany, 2022.

[39] C. J. C. Burges, "A tutorial on support vector machines for pattern recognition," *Data Mining and Knowledge Discovery*, vol. 2, no. 2, pp. 121–167, 1998.

[40] S. Dankwa and W. Zheng, "Special issue on using machine learning algorithms in the prediction of kyphosis disease: a Comparative Study," *Applied Sciences*, vol. 9, no. 16, p. 3322, 2019.

[41] Z. Zhang and L. Wang, "Using Chou's 5-steps rule to identify N^6-methyladenine sites by ensemble learning combined with multiple feature extraction methods," *Journal of Biomolecular Structure and Dynamics*, vol. 40, no. 2, pp. 796–806, 2020.

[42] P. Bulla, L. Anantha, and S. Peram, "Deep neural networks with transfer learning model for brain tumors classification," *Traitement du Signal*, vol. 37, no. 4, pp. 593–601, 2020.

[43] J. Zhang, H. Tang, T. Wen et al., "A hybrid landslide displacement prediction method based on CEEMD and DTW-ACO-SVR—cases studied in the three gorges reservoir area," *Sensors*, vol. 20, no. 15, p. 4287, 2020.

[44] J. Zhang, H. Tang, D. D. Tannant et al., "Combined forecasting model with CEEMD-LCSS reconstruction and the ABC-SVR method for landslide displacement prediction," *Journal of Cleaner Production*, vol. 293, Article ID 126205, 2021.